IEEE Photonics Journal
An IEEE Photonics Society Publication

Open Access

Properties of Rb CPT Atomic Clock at Subharmonic Microwave Modulation Frequencies

Volume 11, Number 4, August 2019

Daba Radnatarov
Sergey Kobtsev, *Member, IEEE*
Valerii Andryushkov
Sergey Khripunov
Evgenii Baklanov
Arkadii Yakovlev

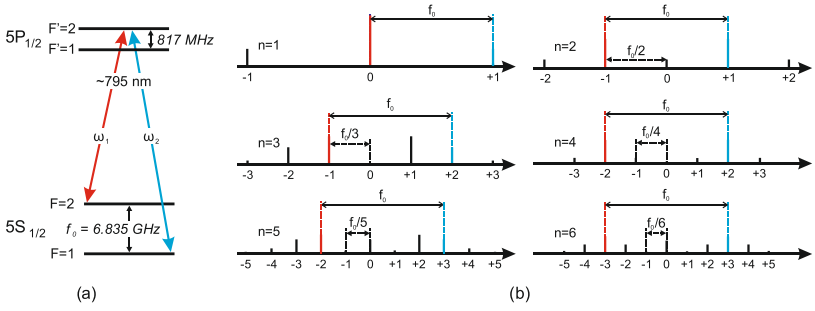

DOI: 10.1109/JPHOT.2019.2925012
1943-0655 © 2019 CCBY

Properties of Rb CPT Atomic Clock at Subharmonic Microwave Modulation Frequencies

Daba Radnatarov,[1] **Sergey Kobtsev**,[1] ***Member, IEEE***, **Valerii Andryushkov**,[1] **Sergey Khripunov**,[1,2] **Evgenii Baklanov**,[3] **and Arkadii Yakovlev**[1]

[1]Division of Laser Physics and Innovative Technologies, Novosibirsk State Universityr, Novosibirsk 630090, Russia
[2]Moscow Institute of Physics and Technology, Dolgoprudny, Moscow region 141700, Russia
[3]Institute of Laser Physics SB RAS, Novosibirsk 630090, Russia

DOI:10.1109/JPHOT.2019.2925012

Manuscript received April 15, 2019; revised June 5, 2019; accepted June 21, 2019. Date of publication June 26, 2019; date of current version July 23, 2019. The work of D. Radnatarov and S. Khripunov (measurement of the experimental data) was supported by a grant of the Russian Scientific Foundation under Project 16-12-10147. The work of S. Kobtsev, E. Baklanov and V. Andryushkov (problem formulation, processing, analysis, and discussion of the generated results) was supported by a grant of the Ministry of Science and Higher Education of the Russian Federation under Project 3.889.2017/PCH. The work of A.Yakovlev (development and fabrication of the used electronic circuits) was supported by a grant of the Russian Foundation for Basic Research under Project 18-29-20025. Corresponding author: Daba Radnatarov (e-mail: d.radnatarov@gmail.com).

Abstract: This letter presents for the first time a systematic study of an atomic frequency standard based on coherent population trapping (CPT) effect in ^{87}Rb vapour optically pumped with a multifrequency laser radiation formed with sidebands of a single-frequency laser whose injection current is modulated at a subharmonic frequency (1/2–1/6) relative to the frequency of hyperfine ground state splitting. Measured are the CPT resonance parameters and the atomic clock short-term stability at different subharmonic frequencies of microwave modulation. The possibility of CPT resonance light shift suppression is experimentally demonstrated at modulation frequencies between 1/3 and 1/5 of the resonant frequency for continuous wave optical pumping of the ^{87}Rb vapour D1 line. Analyzed are the capabilities and potential of reduced energy consumption of atomic clocks when CPT resonance in rubidium vapour is excited at subharmonic modulation frequencies.

Index Terms: Electro-optical systems, novel methods, metrology.

1. Introduction

Coherent population trapping (CPT) effect [1] is widely used in miniaturised high-precision devices, such as atomic clocks [2], [3] and magnetometers [4], [5]. Compact dimensions of equipment based on the CPT effect enables its application in navigation, telecommunication, geo-location, and geodesy. Miniaturisation of CPT-based technology poses new, more stringent requirements to energy consumption and prompts various efforts to reduce it. CPT resonance is formed on hyperfine transitions of the ground state in an alkali atom exposed to bichromatic field created by microwave modulation of the injection current of a vertical-cavity surface-emitting laser (VCSEL) radiating at a frequency close to that of the ground state transition. Energy consumption of the microwave components responsible for generation of the necessary optical sidebands may exceed 50% of the

total energy budget of CPT atomic clock [6], [7]. Therefore, optimisation of the microwave circuit in such devices is very promising in this respect.

It should be noted that there are two major designs of microwave circuits used in atomic clocks. The first relies on frequency multiplication when the microwave modulation frequency is generated from the original 10-MHz clock, while the second involves direct generation of the microwave modulation frequency in acoustic resonators of different types [8]–[11], which is then subdivided in order to obtain the 10-MHz output frequency of the atomic clock. In both cases, a significant amount of energy consumed by the microwave circuit goes to frequency conversion (either from low to high, or *vice versa*). The energy consumption may be reduced by lowering the microwave modulation frequency [12], [13]. This approach is also applicable to RF synthesisers based on integrated circuits [14], [15] and consists in reducing the modulation frequency of the injection current from the value of the hyperfine resonance frequency (HRF, 6.835 GHz) down to one of its subharmonics. Subharmonic modulation leads to formation of sidebands on the optical carrier, several of which are separated by the HRF.

The possibility of using subharmonics of the HRF of an alkali atomic ensemble in order to excite a CPT resonance was earlier demonstrated in [16], [17]. However, these publications did not identify an optimal subharmonic microwave modulation frequency for achievement of the best balance between the energy consumption and the atomic clock stability. In Ref. [16], it was demonstrated in principle that a Rb CPT atomic clock can operate when laser injection current is modulated at the frequency as low as only 1/6 of HRF. Cs-based CPT atomic clocks with even subharmonic modulation only (1/2, 1/4, and 1/6 of HRF) were studied in [17] where CPT resonance parameters were measured, but not the atomic clock stability. Therefore, only fragmentary research has so far been done in this field, which allows neither establishment of the optimal subharmonic frequency for excitation of a CPT resonance nor taking into consideration the possibility of light shit suppression for the CPT resonance at this frequency. Nevertheless, many atomic clocks are modulated at the frequency equal to 1/2 HRF [18]–[21], and this subharmonic has already become a conventional feature.

This work presents for the first time a comparative systematic study of Rb CPT atomic clock (^{87}Rb, D1 line) with laser injection current modulation successively at all HRF subharmonics from 1/2 down to 1/6. We were first of all interested in optimal balance between the energy consumption and atomic clock stability, which would help to improve the performance of modern mass-produced chip-scale atomic clocks.

The present work is organised in the following manner: first, we analyse the methods of CPT resonance excitation *via* multi-frequency radiation (optical sidebands), then we consider the optimal choice of a sideband pair for CPT resonance formation, after which we discuss limitations to lowering the subharmonic frequency and the importance of light shift elimination. Finally, we present the experimental results and discuss them.

2. Analysis of Methods for Multi-Frequency CPT Excitation

2.1 CPT Resonance Excitation With Multi-Frequency Radiation

Division of the working modulation signal frequency by an integer ensures the presence in the laser radiation spectrum of two sidebands, which may participate in excitation of the CPT resonance in a Λ-configuration (Fig. 1). As the microwave modulation frequency is reduced, the resonance will be excited by side components of a higher order. Fig. 1b schematically shows the radiation spectra of a single-frequency semiconductor pump laser whose injection current is modulated at frequencies $f = f_0/n$, where $f_0 = 6.835$ GHz is the frequency of ground state hyperfine splitting in ^{87}Rb (D1 line), $n = 1 \ldots 6$ is the frequency division coefficient.

It can be seen in Fig. 1b that microwave modulation of the laser injection current at fractional frequencies leads to the presence in the multi-frequency spectrum of the laser radiation of two components whose frequency difference equals that of hyperfine ground state splitting, thus ensuring the necessary conditions for excitation of the CPT resonance.

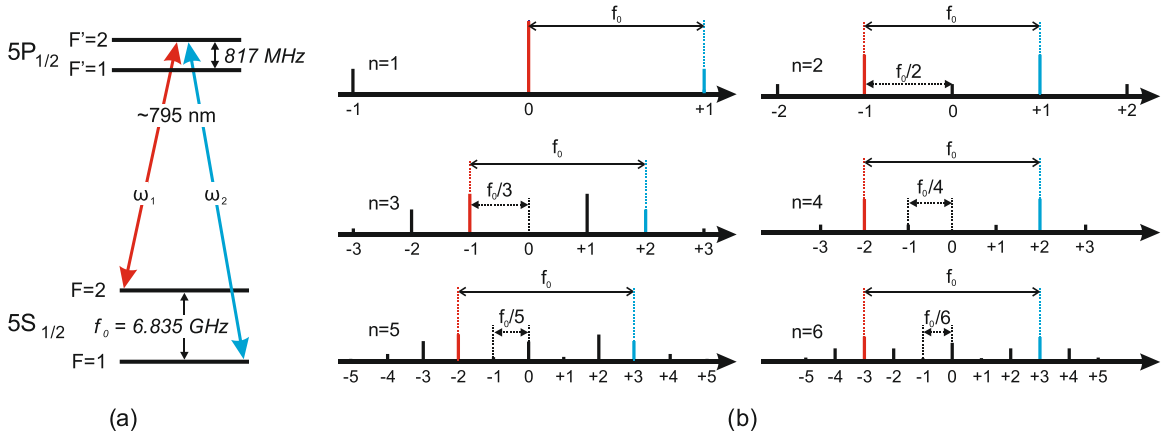

Fig. 1. (a) Level configuration of ^{87}Rb. (b) Schematic laser radiation spectrum when the injection current is modulated at frequency f_0/n, $n = 1 \ldots 6$.

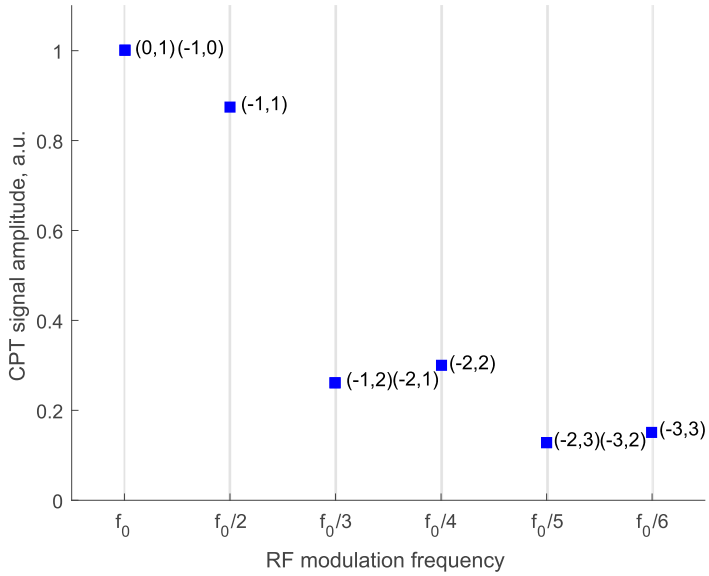

Fig. 2. Maxima of the CPT resonance magnitude at different microwave modulation frequency values, sideband frequency orders given in parentheses.

2.2 Selection of Spectral Components

Sideband frequency magnitude is governed by a Bessel function [22] whose important parameter is the modulation coefficient (index) m representing the modulation depth and indicating the intensity of the impact the modulation signal has upon the carrier. The sideband frequency magnitudes shown in Fig. 1 correspond to the Bessel function values at the modulation parameter m resulting in the highest CPT resonance magnitude, which, in its turn, is proportional to a product of intensities of the chosen sideband frequencies with the frequency difference equal to 6.835 GHz multiplied by their sum [16]. Fig. 2 gives the theoretical values for the CPT resonance magnitudes at different microwave modulation frequencies.

It can be seen in Fig. 2 that the dependence of the CPT resonance magnitude upon the sub-harmonic frequency is not linear, the CPT resonance magnitude at frequency division coefficient $n = 3 \ldots 6$ being substantially lower than those at coefficient $n = 1, 2$. In general, reduction of the

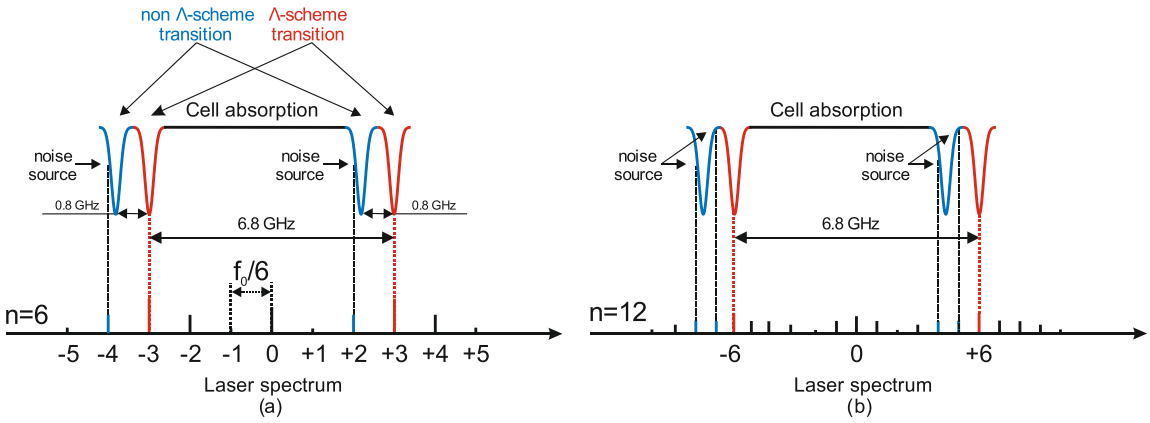

Fig. 3. Interaction of the sideband radiation at n = 6 (a) and n = 12 (b) with ^{87}Rb atomic transitions 5S1/2–5P1/2.

CPT resonance strength at lower subharmonic frequencies is expected, since at lower modulation frequency, the number of sideband frequencies is higher and hence, the laser radiation power is distributed across a greater number of them. However, adjustment of the modulation index m allows a certain degree of control over the process of radiation power distribution among several sideband frequencies. For instance, it is possible to achieve a higher CPT resonance magnitude at the $f_0/4$ subharmonic as compared to modulation at the $f_0/3$ subharmonic, even though the number of sideband frequencies at $f_0/4$ is higher than that existing at $f_0/3$. The same is possible at modulation subharmonic frequencies $f_0/5$ and $f_0/6$.

It can be seen from the calculation results shown in Fig. 2 that the CPT resonance magnitude drops off at lower subharmonic frequencies. This, obviously, should result in worse atomic clock stability. The CPT resonance magnitude may be boosted by increasing the input laser power, but this leads to CPT resonance broadening and also to broader Doppler contour, thus affecting stability. Optimisation of the input laser radiation power in combination with subharmonic microwave modulation requires separate research. Therefore, the present work performs a comparison of CPT resonances at a fixed input laser power.

An important question is which of the existing sideband frequency pairs spaced by 6.835 GHz should be selected from the multi-frequency spectrum, which may contain several such pairs. The optimal set depends on the relationship of transition strengths in the Λ-configuration. In ^{87}Rb, lower-frequency transitions are stronger. Thus, it is more efficient to use the sideband frequency pair where the higher-magnitude component has lower frequency.

As it follows from Fig. 2, the highest CPT resonance magnitudes in the cases of $f = f_0$ and $f = f_0/2$ do not differ much. This is why many researchers use excitation of the CPT resonance at half-frequency $f = f_0/2$ [18]–[21]. This allows to simplify the experimental implementation of their atomic clocks, since a drop in modulation frequency from 6.835 GHz to 3.417 GHz for Rb and from 9.193 GHz to 4.596 GHz for Cs significantly relaxes the minimal parameters of the microwave train and the required modulation bandwidth of the single-frequency semiconductor pump laser.

2.3 Fundamental Limitations on the Lowest Modulation Frequency

As it was noted earlier, lowering the modulation frequency multiplies the number of sideband frequencies. Nevertheless, the accompanying reduction in the radiation power per sideband frequency is not the main factor limiting the lowest achievable modulation frequency. A stronger impact comes from interaction of radiation in the unnecessary sideband frequencies with unused atomic transitions whose frequencies differ from those of the active transitions in the Λ-configuration by 817 MHz (Figs. 1a and 3). This interaction produces additional amplitude noise in the registered spectroscopic

signal, worse signal-to-noise ratio and, consequently, a drop in the atomic clock stability. Typical spectral width of these spurious absorption lines at the working temperature of the optical cell is around ~530 MHz [23]. Therefore, noticeable absorption of the sideband frequency radiation by these lines occurs when the frequency of the closest unused sideband is spaced from the frequency of the working sideband by an amount below 817 MHz + 530/2 MHz = 1082 MHz. Considering broad absorption line wings, this effect becomes important at the sideband frequency difference of ~1.2–1.4 GHz. For the D1 line in ^{87}Rb, this effect manifests itself noticeably at subharmonic modulation with $f_0/5 = 1.367$ GHz, $f_0/6 = 1.139$ GHz and lower.

For the D1 line in ^{133}Cs, the frequencies of "parasitic" transitions differ by 1.168 GHz. Hence, with the widths of these lines taken into account and their broad wings, the lowest practical modulation frequency in this case corresponds to the subharmonic at frequency $f_0/5 = 1.838$ GHz.

It should be mentioned that the analysis given above is also valid for cells with buffer gas, taking into account the fact that in such cells, the Doppler contour width at the working buffer gas pressure may be within 1–2 GHz [24]. Because of the greater absorption line width in cells with buffer gas, the lowest practical modulation frequency for them is higher, around $f_0/3$–$f_0/4$. We tend to believe that the choice of the cell type (buffer-gas or wall-coated cell) did not play a critical role in the present study because it was shown earlier [25] that both types of cells deliver similar stability of CPT atomic clock at the same cell dimensions. We used wall coating because such cells allow comparison of atomic clock parameters in a broader range of subharmonics.

2.4 Elimination of Light Shift in the CPT Resonance Excited With Multi-Frequency Radiation

Light shift of atomic levels caused by interaction of atoms with the pumping radiation makes a significant contribution to instability of the spectral position of the excited CPT resonance [26]–[30]. However, optimisation of the pump radiation power may be used to minimise the light shift in the CPT resonance [31]. Up to date, such possibility was demonstrated at modulation frequencies equal to f_0 and $f_0/2$. Rather obviously, the problem of light shift suppression is also important in studies of CPT atomic clocks modulated at lower subharmonics. This work will pay special attention to this.

3. Experimental Setup

The studied experimental set-up is schematically represented in Fig. 4. The conventional atomic clock architecture was used [32]: a CPT resonance at the D1 line in ^{87}Rb was formed with the help of two-frequency radiation and was further used for improvement of long-term stability of a local oscillator. In order to generate the required two-component radiation with the specific frequency difference corresponding to the transition frequency between the sub-levels of hyperfine ^{87}Rb ground level splitting, the injection current of a single-frequency VCSEL with a linewidth of 50 MHz emitting at 795 nm was modulated at 3.417 GHz, resulting in generation of sidebands with the frequency difference of 6.835 GHz. The CPT resonance was scanned by variation of this frequency difference around the HRF at frequency of 2 kHz and amplitude of 1 kHz. As it was shown earlier [33], [34], this relationship between the modulation frequency and amplitude (2:1) results in the best achievable stability of atomic clock. The CPT resonance on transitions between magnetically insensitive levels ($m_F = 0$) was excited with circularly polarised radiation [35]. The temperature of the 10-mm cubic cell containing ^{87}Rb vapour was kept at 60 °C, while its internal walls had an anti-relaxation paraffine coating. The cell was also placed inside a 3-layer μ-metal shield in order to protect it from external magnetic fields. A pair of Helmholtz coils was used to create a longitudinal magnetic field with induction strength of around 100 mG for splitting of magnetic sub-levels. In addition to the primary feed-back loop for stabilisation of the local oscillator frequency, an auxiliary feed-back loop was also used for locking the laser's output wavelength to the ^{87}Rb absorption line [36]. Modulation frequencies of these two loops were chosen not to be multiples of each other (2 kHz and 10.1 kHz) in order to prevent one of the loops from affecting the other. The VCSEL

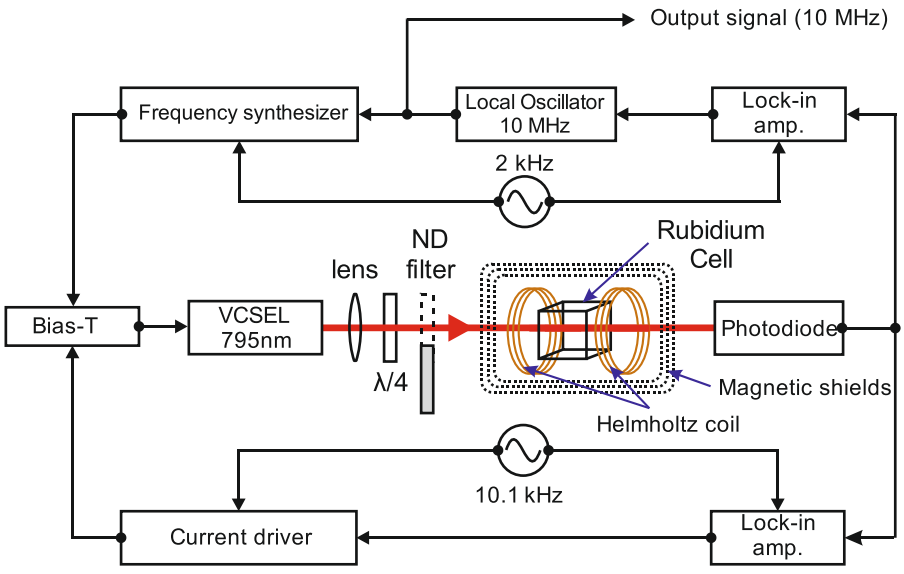

Fig. 4. Experimental set-up.

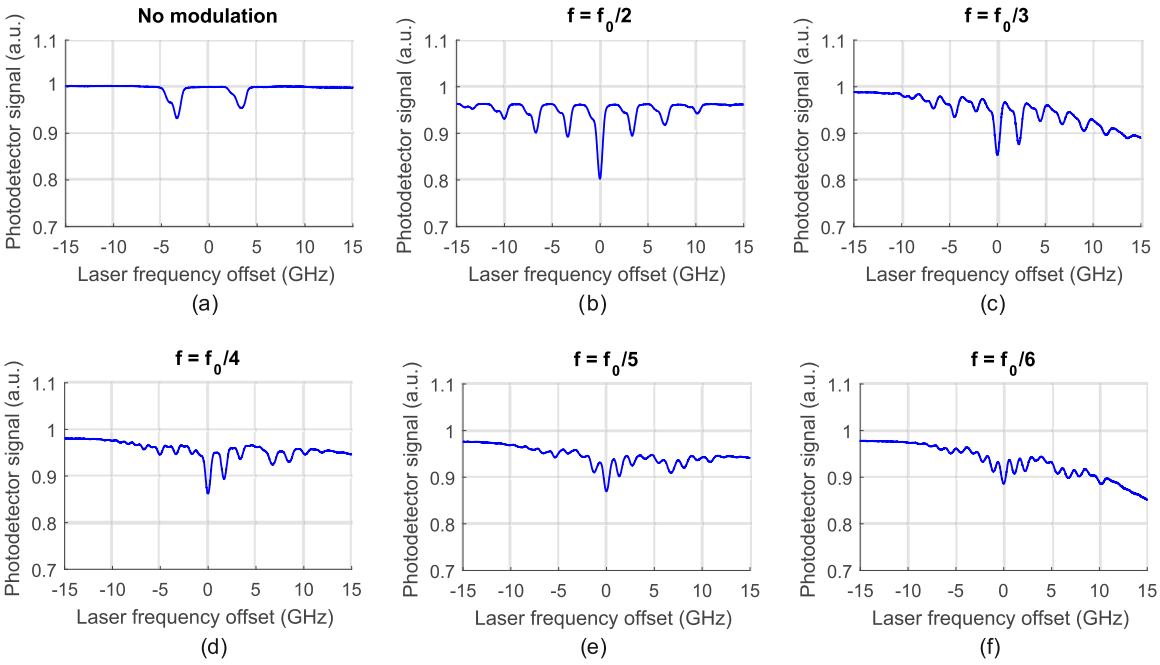

Fig. 5. Absorption spectra of ^{87}Rb in the optical cell: (a) in the absence of microwave modulation; at the frequency of microwave modulation equal to (b) $f_0/2$, (c) $f_0/3$, (d) $f_0/4$, (e) $f_0/5$, (f) $f_0/6$.

output power was 55 μW, and the beam diameter within the optical cell was 1.5 mm. The light shift amount was measured by reducing the pumping power down to 25 μW with a neutral-density filter.

4. Results and Discussion

Fig. 5 shows absorption spectra of ^{87}Rb vapours in the cell both without the laser injection current modulation (Fig. 5a) and with the injection current modulated at different frequencies (Fig. 5b–5f).

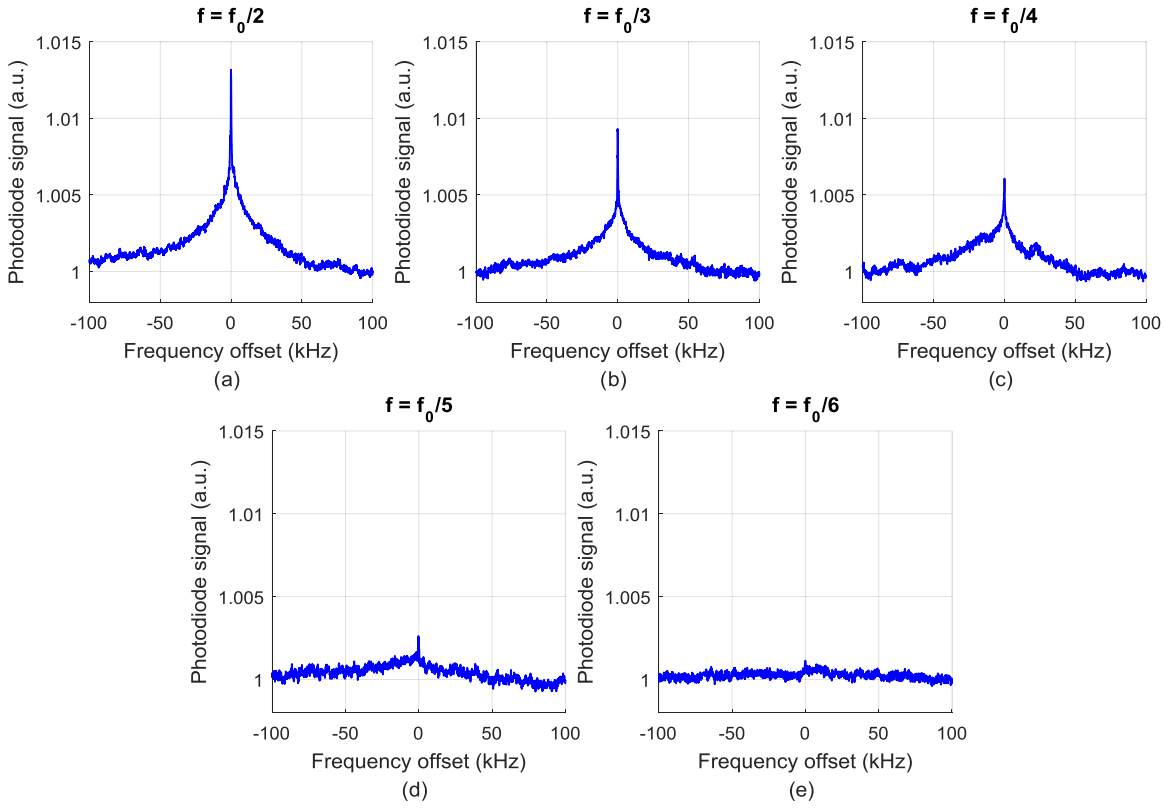

Fig. 6. CPT resonances under microwave modulation at frequencies: (a) $f_0/2$, (b) $f_0/3$, (c) $f_0/4$, (d) $f_0/5$, (e) $f_0/6$.

These spectra were registered with a photodiode, and the laser output wavelength was scanned by adjustment of the DC component of the injection current. In the absence of modulation, the transmission spectrum (Fig. 5a) features two absorption peaks separated by 6.835 GHz. Each peak is formed by two unresolved absorption lines with 817 MHz between their centres. These absorption lines correspond to transitions onto different sub-levels of the upper $5P_{1/2}$ level of the D1 line in ^{87}Rb (see Fig. 1a) and they merge because of Doppler broadening. Modulation of the injection current of the pumping laser results in emergence in the laser output spectrum of additional spectral components (sideband frequencies). Correspondingly, this leads to more absorption peaks in the transmission spectrum (Fig. 5b–5f). It can be seen that lower modulation frequency corresponds to smaller absorption peak separation and their amplitude because of distribution of the laser radiation power among a larger number of sidebands.

Fig. 6 presents CPT resonance shapes at modulation frequencies f_0/n, where $n = 2 \ldots 6$. It can be seen that the CPT resonance contrast becomes expectedly worse at lower modulation frequency and that at $f_0/6$, the resonance cannot be distinguished from the noise background. The contrast was traditionally defined as the ratio of the resonance magnitude to that of the resonance base line. The resonances measured at $n = 2 \ldots 4$ feature a dual structure typical for cells with anti-relaxation coating [37]. At odd values of n, CPT resonance is formed by atomic interactions with sideband frequencies positioned asymmetrically with respect to the carrier. The best CPT resonance contrast at $f_0/3$ was produced by sideband components "–1" and "+2", while the best contrast at $f_0/5$ corresponded to components "–2" and "+3" (Fig. 1). As it was mentioned above, this results from different absorption cross-section (relative hyperfine transition strength factors) of the transitions participating in the Λ-configuration (Fig. 5a) and from the distribution of the pumping radiation among the sideband components.

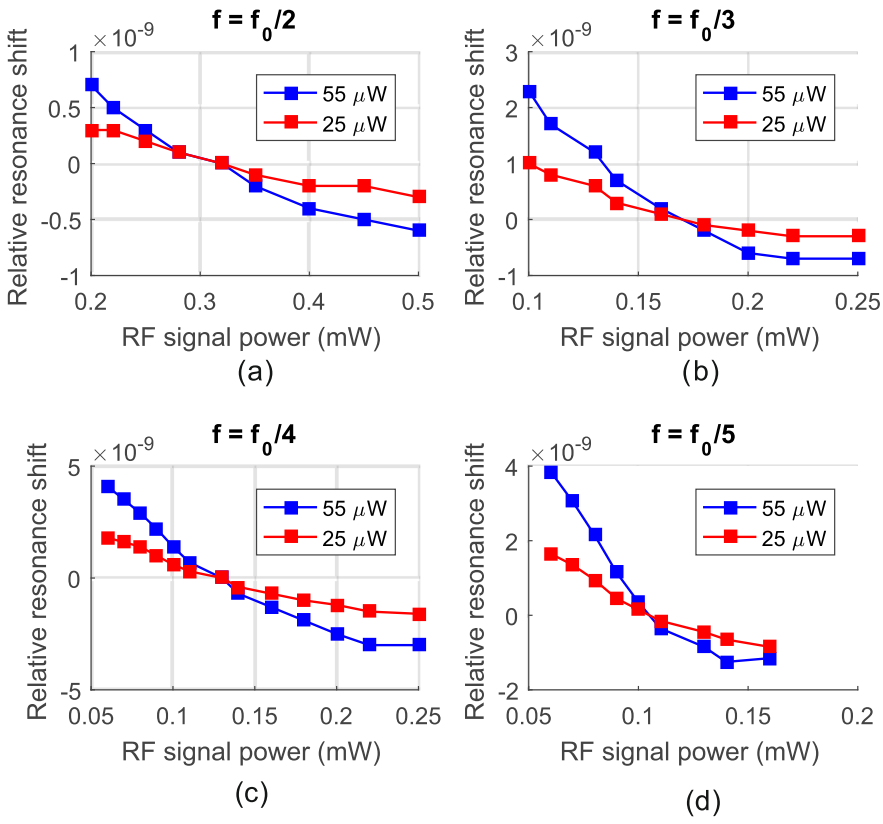

Fig. 7. Dependence of the CPT resonance shift upon the power of the microwave signal at the laser output power equal to 55 μW (blue squares) and 25 μW (red squares) for different modulation frequencies: (a) $f_0/2$, (b) $f_0/3$, (c) $f_0/4$, (d) $f_0/5$.

Adjustment of the power of the microwave signal added to the laser injection current (Fig. 7) not only affects distribution of the radiation power among the sidebands, but also allows suppression of light shift of the CPT resonance [38], [39]. Shown in Fig. 7 are dependencies of the CPT resonance shift upon the microwave signal power at two different laser output power levels, 25 and 55 μW. The point where the two dependencies cross corresponds to the microwave signal power, at which the light shift of the CPT resonance is eliminated. In the vicinity of this point, the position of the CPT resonance does not depend on the radiation intensity. Therefore, we have experimentally demonstrated that light shift of the CPT resonance can be suppressed at fractional modulation frequencies f_0/n, where $n = 3 \ldots 5$.

It follows from Fig. 7 that the microwave signal power necessary for suppression of light shift decreases with the modulation frequency, even though in general, the microwave signal power should increase as the modulation frequency is reduced in order to ensure the same power at the spectral components spaced by 6.835 GHz. This happens because efficiency of the laser current modulation drops at higher frequencies. Correspondingly, higher RF signal power becomes necessary in order to ensure the same RF modulation depth at a higher RF modulation frequency.

Parameters of the studied atomic clocks at different modulation frequencies are summarised in Table 1. Energy consumption of the microwave circuit was calculated in the approximation of its linear dependence upon the RF signal frequency [12], [13]. This approximation was chosen, considering the fact that the RF signal power ($<$1 mW) is small and amounts to few per cent relative to the total consumption of the microwave train (40–50 mW).

Table 1 demonstrates that both contrast and width of CPT resonances drop off at lower modulation frequencies, which leads to greater instability of the atomic clock frequency. However, at lower

TABLE 1
Atomic Clock Parameters at Different Modulation Frequencies

Symbol	$f_0/2$	$f_0/3$	$f_0/4$	$f_0/5$
f (GHz)	3.417	2.278	1.708	1.366
Sideband order	–1 & +1	–1 & +2	–2 & +2	–2 & +3
Consumption / K_1	1 / 1	0.67 / 1.5	0.5 / 2.0	0.4 / 2.5
Contrast (%)	1.3	0.9	0.6	0.3
FWHM (kHz)	1.64	1.59	1.44	1.40
ADEV / K_2	4.3 / 1	4.8 / 1.1	7.1 / 1.7	10.5 / 2.4
$A=K_1/K_2$	1	**1.36**	1.18	1.04

Consumption – calculated energy consumption of the microwave synthesiser (a.u.); Contrast – CPT resonance contrast; FWHM – CPT resonance width; A – energy efficiency parameter of the microwave circuit; ADEV – Allan deviation σ_y ($\tau = 1$ sec) $\times 10^{-11}$.

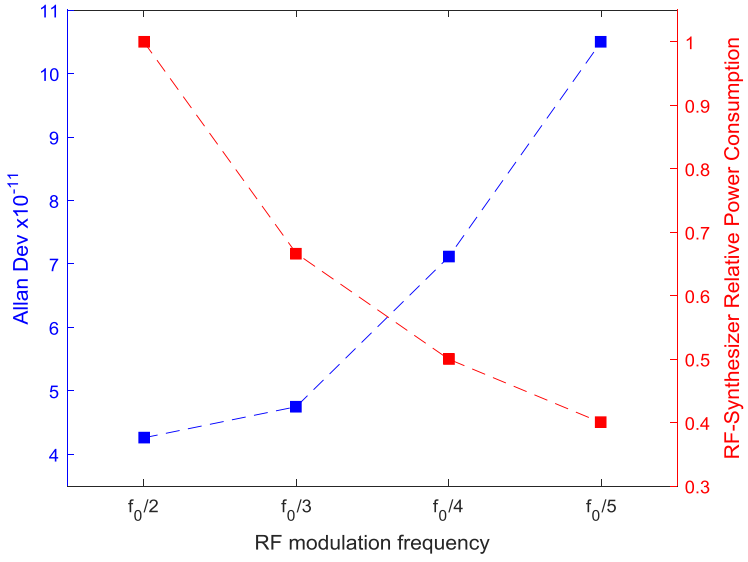

Fig. 8. Experimental dependencies of atomic clock stability over 1 s and calculated energy consumption of the microwave synthesiser upon the RF modulation frequency.

modulation frequency, the power consumption of the microwave train is also reduced. In order to determine the optimal combination of the atomic clock stability and power consumption, we introduced the energy efficiency parameter $A = K_1/K_2$. Here, K_1 is the consumption reduction coefficient, $K_1 = P_0/P_n$, where P_0 is the energy consumption of the microwave train at the modulation frequency $f_0/2$ and P_n is consumption at modulation frequencies f_0/n, where $n = 2 \ldots 5$, and K_2 is the instability growth coefficient relative to instability at the modulation frequency $f_0/2$. $K2 = ADEV_n/ADEV_0$, where $ADEV_n$ is Allan deviation at modulation frequencies f_0/n ($n = 2 \ldots 5$), $ADEV_0$ is Allan deviation at the modulation frequency $f_0/2$. Allan deviation was measured with a frequency comparator having a built-in frequency reference with its own instability of 4×10^{-12} over 1 second.

Table 1 shows that the energy efficiency parameter A reaches a maximum at the modulation frequency $f_0/3$, after that it begins to drop off as the modulation frequency is further reduced. It is

pertinent to point out that despite parameter A being artificial, it allows a quantitative comparison of atomic clocks at different modulation frequencies.

Fig. 8 lays out experimental dependencies of the atomic frequency standard stability over 1 second and calculated energy consumption of the microwave synthesiser upon the modulation frequency. As it follows from Fig. 8, these dependencies exhibit opposite behaviour and cross at a point between modulation frequencies $f_0/3$ and $f_0/4$. The performance is better at modulation frequency $f_0/3$: the atomic clock stability drop is relatively small (11%), while the energy consumption of the microwave synthesizer is 1.5 times lower.

Let us note that comparison of atomic clock parameters corresponding to different modulation frequencies was performed at a fixed incident radiation power, even though it may be adjusted to optimise short-term stability of the studied atomic clock. We did all measurements at a single level of radiation power in order to better isolate the specific effect the modulation frequency has on short-term stability of the clock.

It would be interesting, as well, to explore the influence of lower modultation frequencies upon long-term stability of atomic clocks. However, clock stability over longer periods (for example over 24 hours or longer) does not as much depend on the modulation parameters as it does upon other ones (temperature stability, shielding of the cell from magnetic fields, etc.).

5. Conclusion

This work has for the first time studied the properties of CPT-based atomic clocks with continuous-wave optical pumping of the ^{87}Rb vapour D1 line in a compact cell and higher-order sideband excitation of the CPT resonance. The degree of atomic clock stability (Allan deviation) drop with increasing subharmonic order was identified. The evolution of stability was analysed in relation to energy consumption of the microwave synthesiser and the optimal parameter of energy efficiency was determined, at which the minimal drop in stability is accompanied by the maximal reduction in energy consumption of the microwave synthesiser. This parameter is optimal for the modulation frequency $f_0/3$, at which the atomic clock stability drops only slightly (by 11%), whereas the energy consumption of the microwave synthesiser is reduced by a factor of 1.5. For modulation frequencies f_0/n, where $n = 3 \ldots 5$, it was demonstrated that light shift can be eliminated at continuous-wave optical pumping of the D1 line of ^{87}Rb vapour in a compact cell.

Adoption of modulation at frequency $f_0/3$ will significantly reduce energy consumption of the microwave synthesiser at the cost of only slight drop in the atomic clock stability for any type of microwave synthesisers implemented with either discrete components, integrated circuits [14], [15], or with bulk resonators [8]–[11].

The results of the presented study open up a new possibility for performance improvement in compact CPT atomic devices (clocks, magnetometers, gyroscopes) relying on different microwave circuit design both with frequency multiplication and frequency division. Reduction in the microwave modulation frequency also relaxes the requirements to the VCSEL modulation bandwidth. It is important to point out that practical implementation of the identified possibility of performance improvements in compact atomic clocks does not entail significant modification of their design.

References

[1] E. Arimondo, "V Coherent population trapping in laser spectroscopy," *Prog. Opt.*, vol. 35, pp. 257–354, Dec. 1996.
[2] J. Vanier, "Atomic clocks based on coherent population trapping: A review," *Appl. Phys. B*, vol. 81, no. 4, pp. 421–442, Aug. 2005.
[3] S. Knappe *et al.*, "A chip-scale atomic clock based on ^{87}Rb with improved frequency stability," *Opt. Exp.*, vol. 13, no. 4, pp. 1249–1253, Feb. 2005.
[4] A. Nagel *et al.*, "Experimental realization of coherent dark-state magnetometers," *Europhys. Lett.*, vol. 44, no. 1, pp. 31–36, Oct. 1998.
[5] P. D. D. Schwindt, S. Knappe, V. Shah, L. Hollberg, and J. Kitching, "Chip-scale atomic magnetometer," *Appl. Phys. Lett.*, vol. 85, no. 26, pp. 6409–6411, Dec. 2004.

[6] R. Lutwak, P. Vlitas, M. Varghese, M. Mescher, D. K. Serkland, and G. M. Peake, "The MAC - A miniature atomic clock," in *Proc. IEEE Int. Freq. Control Symp. Expo.*, Aug. 2005, pp. 752–757.

[7] R. Lutwak, "The chip-scale atomic clock - recent developments," in *Proc. IEEE Int. Freq. Control Symp. Joint 22nd Eur. Freq. Time Forum*, Apr. 2009, pp. 573–577.

[8] A. Artieda and P. Muralt, "3.4 GHz composite thin film bulk acoustic wave resonator for miniaturized atomic clocks," *Appl. Phys. Lett.*, vol. 98, no. 26, Jun. 2011, Art. no. 262902.

[9] M. Hara *et al.*, "Microwave oscillator using piezoelectric thin-film resonator aiming for ultraminiaturization of atomic clock," *Rev. Sci. Instrum.*, vol. 89, no. 10, Oct. 2018, Art. no. 105002.

[10] T. Daugey, J.-M. Friedt, G. Martin, and R. Boudot, "A high-overtone bulk acoustic wave resonator-oscillator-based 4.596 GHz frequency source: Application to a coherent population trapping Cs vapor cell atomic clock," *Rev. Sci. Instrum.*, vol. 86, no. 11, Nov. 2015, Art. no. 114703.

[11] H. Yu *et al.*, "HBAR-based 3.6 GHz oscillator with low power consumption and low phase noise," *IEEE Ultrason. Ferrelectr.*, vol. 56, no. 2, pp. 400–403, Feb. 2009.

[12] A. S. Sedra and K. C. Smith, *Microelectronic Circuits*. London, U.K.: Oxford Univ. Press, 2014.

[13] M. Kumar, "A low power voltage controlled oscillator design," *ISRN Electron.*, vol. 2013, May 2013, Art. no. 987179.

[14] Y. Zhao *et al.*, "A 15 mW, 4.6 GHz frequency synthesizer ASIC with −85 dBc/Hz at 2 kHz for miniature atomic clocks," in *Proc. Joint Conf. IEEE Int. Freq. Control Eur. Freq. Time Forum*, Jul. 2013, pp. 715–717.

[15] S. Pellerano, S. Levantino, C. Samori, and A. L. Lacaita, "A 13.5-mW 5-GHz frequency synthesizer with dynamic-logic frequency divider," *IEEE J. Solid-State Circuits*, vol. 39, no. 2, pp. 378–383, Feb. 2004.

[16] N. Cyr, M. Tetu, and M. Breton, "All-optical microwave frequency standard: A proposal," *IEEE Trans. Instrum. Meas.*, vol. 42, no. 2, pp. 640–649, Apr. 1993.

[17] S. Goka and Y. Yano, "Higher-order sideband excitation method for pulsed CPT atomic clock," in *Proc. Joint Eur. Freq. Time Forum Int. Freq. Control Symp.*, Jul. 2013, pp. 228–231.

[18] S. Knappe, V. Shah, P. D. D. Schwindt, L. Hollberg, and J. Kitching, "A microfabricated atomic clock," *Appl. Phys. Lett.*, vol. 85, no. 9, pp. 1460–1462, Aug. 2004.

[19] Z. Wang, "Review of chip-scale atomic clocks based on coherent population trapping," *Chin. Phys. B*, vol. 23, no. 3, Mar. 2014, Art. no. 030601.

[20] M. Kajita, "The fundamentals of an atomic clock," in *Measuring Time: Frequency Measurements and Related Developments in Physics*. Bristol, U.K.: IOP, 2018.

[21] J. Kitching, "Chip-scale atomic devices," *Appl. Phys. Rev.*, vol. 5, no. 3, Sep. 2018, Art. no. 031302.

[22] B. Van Der Pol, "Frequency modulation," *Proc. Inst. Radio Eng.*, vol. 18, no. 7, pp. 1194–1205, Jul. 1930.

[23] W. Demtröder, *Laser Spectroscopy: Basic Concepts and Instrumentation*, 3rd ed. New York, NY, USA: Springer, 2013.

[24] G. A. Pitz, A. J. Sandoval, T. B. Tafoya, W. L. Klennert, and D. A. Hostutler, "Pressure broadening and shift of the rubidium D_1 transition and potassium D_2 transitions by various gases with comparison to other alkali rates," *J. Quant. Spectrosc. Radiat. Transf.*, vol. 140, pp. 18–29, Jun. 2014.

[25] J. Kitching, S. Knappe, and L. Hollberg, "Miniature vapor-cell atomic-frequency references," *Appl. Phys. Lett.*, vol. 81, no. 3, pp. 553–555, Jul. 2002.

[26] E. B. Aleksandrov, A. M. Bonch-Bruevich, N. N. Kostin, and V. A. Khodovoi, "Frequency shift of optical transition in the field of a light wave," *JETP Lett.*, vol. 3. pp. 53–55, Jan. 1966.

[27] A. M. Bonch-Bruevich, N. N. Kostin, V. A. Khodovoi, and V. V. Khromov, "Changes in the atomic absorption spectrum in the field of a light wave I," *Sov. J. Exp. Theor. Phys.*, vol. 29, no. 1, pp. 82–85, Jul. 1969.

[28] A. Nagel, S. Brandt, D. Meschede, and R. Wynands, "Light shift of coherent population trapping resonances," *Europhys. Lett.*, vol. 48, no. 4, pp. 385–389, Nov. 1999.

[29] N. Delone and V. Krainov, "AC stark shift of atomic energy levels," *Phys.-Uspekhi*, vol. 42, no. 7, pp. 669–689, Jul. 1999.

[30] V. Gerginov, S. Knappe, V. Shah, P. D. D. Schwindt, L. Hollberg, and J. Kitching, "Long-term frequency instability of atomic frequency references based on coherent population trapping and microfabricated vapor cells," *J. Opt. Soc. Amer. B*, vol. 23, no. 4, pp. 593–597, Apr. 2006.

[31] M. Zhu and L. S. Cutler, "Theoretical and experimental study of light shift in a CPT-based Rb vapor cell frequency standard," in *Proc. 32nd Annu. Precise Time Time Interval Syst. Appl. Meeting*, Nov. 2000, pp. 311–322.

[32] S. Khripunov, D. Radnatarov, and S. Kobtsev, "Atomic clock based on a coherent population trapping resonance in ^{87}Rb with improved high-frequency modulation parameters," *Proc. SPIE*, vol. 9378, Mar. 2015, Art. no. 93780A.

[33] I. Ben-Aroya, M. Kahanov, and G. Eisenstein, "Optimization of FM spectroscopy parameters for a frequency locking loop in small scale CPT based atomic clocks," *Opt. Exp.*, vol. 15, no. 23, pp. 15060–15065, Oct. 2007.

[34] S. M. Kobtsev, D. Radnatarov, S. Khripunov, I. Popkov, V. Andryushkov, and T. Steschenko, "Atomic clock stability under dynamic excitation of coherent population trapping resonance in cells without buffer gas," *Proc. SPIE*, vol. 10548, Feb. 2018, Art. no. 1054820.

[35] V. Shah and J. Kitching, "Advances in coherent population trapping for atomic clocks," in *Advances in Atomic, Moleculer, and Optical Physics*, vol. 59, E. Arimondo, P. R. Berman, and C. C. Lin, Eds. Amsterdam, The Netherlands: Elsevier, 2010, pp. 21–74.

[36] F. Riehle, *Frequency Standards: Basics and Applications*. Hoboken, NJ, USA: Wiley, 2004.

[37] E. Breschi *et al.*, "Light effects in the atomic-motion-induced Ramsey narrowing of dark resonances in wall-coated cells," *Phys. Rev. A*, vol. 82, no. 6, Dec. 2010, Art. no. 063810.

[38] F. Levi, A. Godone, and J. Vanier, "The light shift effect in the coherent population trapping cesium maser," *IEEE Ultrason. Ferroelectr.*, vol. 47, no. 2, pp. 466–470, Mar. 2000.

[39] S. Kobtsev *et al.*, "Feedback-controlled and digitally processed coherent population trapping resonance conversion in ^{87}Rb vapour to high-contrast resonant peak," *New J. Phys.*, vol. 19, no. 4, Apr. 2017, Art. no. 043016.